Mutations in the 'DRY' motif of the CB_1 cannabinoid receptor result in biased receptor variants

Pál Gyombolai[1,2], András D. Tóth[1], Dániel Tímár[1], Gábor Turu[1], László Hunyady[1,2,#]

[1]Department of Physiology, Faculty of Medicine, Semmelweis University, Budapest, Hungary, gyombolai.pal@med.semmelweis-univ.hu, toth.andras1@med.semmelweis-univ.hu, timar.daniel.sote@gmail.com, turu.gabor@med.semmelweis-univ.hu

[2]MTA-SE Laboratory of Molecular Physiology, Hungarian Academy of Sciences and Semmelweis University, Budapest, Hungary

[#]Address correspondence to: Prof. Dr. László Hunyady, Department of Physiology, Faculty of Medicine, Semmelweis University, H-1444 Budapest, P. O. Box 259, Hungary, Fax: 36-1-266-6504, Phone: 36-1-266-9180, E-mail: Hunyady@puskin.sote.hu

Short title: Mutations in the 'DRY' motif of CB_1 receptor

Keywords: G proteins, Signal transduction, Mutations, Receptors

Word count: 5456

Abstract

The role of the highly-conserved 'DRY' motif in the signaling of the CB_1 cannabinoid receptor (CB_1R) was investigated by introducing single, double and triple alanine mutations into this site of the receptor. We found that the CB_1R-R3.50A mutant displays a partial decrease in its ability to activate heterotrimeric G_o proteins (~80% of wild-type CB_1R (CB_1R-WT)). Moreover, this mutant showed an enhanced basal β-arrestin2 recruitment. More strikingly, the double mutant CB_1R-D3.49A/R3.50A was biased toward β-arrestins, as it gained a robustly increased β-arrestin1 and β-arrestin2 recruitment ability compared to the wild-type receptor, while its G protein activation was decreased. In contrast, the double mutant CB_1R-R3.50A/Y3.51A proved to be G protein-biased, as it was practically unable to recruit β-arrestins in response to agonist stimulus, while still activating G proteins, although at a reduced level (~70% of CB_1R-WT). Agonist-induced ERK1/2 activation of the CB_1R mutants showed good correlation with their β-arrestin recruitment ability but not with their G protein activation or inhibition of cAMP accumulation. Our results suggest that G protein activation and β-arrestin binding of the CB_1R are mediated by distinct receptor conformations and the conserved 'DRY' motif plays different roles in the stabilization of these conformations, thus mediating both G protein- and β-arrestin-mediated functions of CB_1R.

1. Introduction

Seven transmembrane receptors (7TMRs) constitute the largest family of plasma membrane receptors. Most of their intracellular effects are mediated via direct coupling to heterotrimeric G proteins. To understand the molecular details of 7TMR activation and G protein coupling, identification of key structural elements regulating these processes is critically important. Using mutational analyses as well as recent high resolution X-ray crystal structure data, such structural features have been extensively mapped (Venkatakrishnan et al. 2013). Among these, the conserved Asp-Arg-Tyr (DRY) motif, located at the beginning of the second intracellular loop (ICL2), seems to play a central role both in the activation and the G protein coupling of class A (rhodopsin-like) 7TMRs (Rasmussen et al. 2011). Nevertheless, the exact nature of this regulatory role is still not completely understood. For instance, although the Arg residue (R3.50) is suggested to directly interact with the G protein α subunit in the active 7TMR conformation, its non-conservative mutations in many cases fail to impair G protein coupling of the receptor (Fanelli et al. 1999; Rhee et al. 2000; Rovati et al. 2007). Furthermore, Asp (D3.49) is believed to stabilize inactive receptor conformation by forming a salt-bridge with the neighboring R3.50 (Scheer et al. 1996; Scheer et al. 1997; Ballesteros et al. 1998; Ballesteros et al. 2001; Li et al. 2001), however, its mutations can also result in completely diverse phenotypes, depending on the investigated receptor (Rovati et al. 2007). Therefore, the exact role of the DRY motif obviously shows receptor-specific differences, and its detailed analysis for a particular 7TMR seems reasonable.

Besides G proteins, β-arrestins are also able to directly bind to the intracellular surface of an activated 7TMR, leading to the desensitization and internalization of the receptor (Shenoy and Lefkowitz 2011). Moreover, receptor-bound β-arrestins can also serve as a starting point for G protein-independent signaling pathways, such as the activation of the p42/44 mitogen-activated protein kinase (MAP kinase) cascade or Src kinases (Wei et al. 2003; DeWire et al. 2007).

Many data suggest that the β-arrestin-bound conformation of 7TMRs may differ from the one mediating their G protein activation, a fact being implicitly exploited by several functionally selective 7TMR ligands as well as by functionally selective 7TMR mutants, which are able to induce β-arrestin recruitment without affecting G protein coupling or vice versa (Reiter et al. 2012). However, in the lack of a high resolution crystal structure describing a 7TMR in its β-arrestin-bound form, relatively little is known about the receptor-arrestin binding interface. According to the prevailing idea, arrestins utilize two distinct sites to bind to 7TMRs, one of which is a ‘phosphorylation sensor’, recognizing Ser/Thr-phosphorylated C-terminus of the receptor (Gurevich and Benovic 1993; Gurevich and Gurevich 2006). The other site is a so-called ‘activation sensor’, which recognizes the active 7TMR conformation, independently of receptor phosphorylation (Gurevich and Gurevich 2006). The 7TMR elements constituting the docking site for the arrestin ‘activation sensor’ are less understood. The second intracellular loop (ICL2), beginning with the DRY motif, has been proposed to play such a role (Huttenrauch et al. 2002; Marion et al. 2006). Furthermore, complementary roles for the DRY motif and receptor C-terminus in the regulation of β-arrestin binding have been described (Kim and Caron 2008). In addition, mutations of R3.50 in many cases results in basal β-arrestin

86 binding and subsequent constitutively desensitized phenotype of 7TMRs (Barak et al.
87 2001; Wilbanks et al. 2002). Thus, the conserved DRY motif seems to be involved not
88 only in G protein coupling, but also in β-arrestin binding of 7TMRs.
89 The CB_1 cannabinoid receptor (CB_1R) belongs to the 7TMR superfamily. The signaling
90 pathways originating from CB_1R are mediated mainly via heterotrimeric $G_{i/o}$ proteins,
91 and include inhibition of cAMP production, activation of GIRK potassium channels,
92 inhibition of Ca_v calcium channels, and activation of MAP kinase cascades (Turu and
93 Hunyady 2010). Moreover, CB_1R shows basal G protein activation and constitutive
94 internalization under diverse cellular conditions (Leterrier et al. 2006; McDonald et al.
95 2007; Turu et al. 2007). Like most other 7TMRs, CB_1R also recruits β-arrestin following
96 activation, which leads to the desensitization and internalization of the receptor
97 (Kouznetsova et al. 2002; Daigle et al. 2008; Gyombolai et al. 2013). The binding
98 between β-arrestins and CB_1R is relatively weak, and the affinity of the receptor for β-
99 arrestin2 (β-arr2) is substantially higher than that for β-arrestin1 (β-arr1) (Gyombolai et
100 al. 2013). Furthermore, β-arr1 recruitment of CB_1R appears to be agonist-dependent
101 (Laprairie et al., 2014; Flores-Otero et al., 2014). Interestingly, in addition to canonical G
102 protein-mediated intracellular effects, recent data suggest the existence of β-arrestin-
103 mediated, G protein-independent signaling of CB_1R, i.e. the p42/44 MAPK (ERK1/2)
104 activation of the receptor seems to be at least partly mediated by β-arrestins (Ahn et al.
105 2013a; Mahavadi et al. 2014).
106 Via these cellular events, CB_1R is involved in the regulation of many important
107 physiological and pathophysiological processes, such as memory, learning, pain
108 sensation, metabolic regulation, or the regulation of vascular tone (Pacher et al. 2006).

109 Moreover, several natural and synthetic cannabinoid ligands are known to stabilize
110 distinct active CB_1R conformations, i.e. prove to be functionally selective (Glass and
111 Northup 1999; Mukhopadhyay and Howlett 2001; Ahn et al. 2013a). Thus, investigation
112 of the structural elements responsible for G protein- and β-arrestin-mediated CB_1R
113 functions has a major physiological and pharmacological impact. Accordingly, a number
114 of studies have aimed to identify such regulatory motifs of CB_1R. A detailed
115 computational model based on the crystal structure of the β_2-adrenergic receptor-$G\alpha_s$
116 complex, combined with mutational data, suggested that distinct residues in the ICL2 and
117 ICL3 regions of the CB_1R may be involved in the stabilization of the active, $G\alpha_i$-coupled
118 receptor conformation (Shim et al. 2013). Two other recent studies analyzed the role of
119 several intramolecular salt-bridges, which may stabilize inactive, partially active and
120 fully active CB_1R conformations (Ahn et al. 2013b; Scott et al. 2013). According to this
121 model, D3.49 and R3.50 residues form salt-bridges with K4.41 and D6.30, respectively,
122 which (together with a D2.63+K3.28 salt-bridge) may keep the receptor in a partially
123 active conformation under basal conditions.
124 Less is known about the structural features governing the β-arrestin binding of CB_1R. The
125 C-terminal Ser/Thr phosphorylation of the receptor seems to play a role, since alanine
126 mutations of these residues impaired agonist-induced β-arrestin recruitment and
127 subsequent internalization of CB_1R (Daigle et al. 2008).
128 Although the above studies clearly provide important insights into the molecular details
129 of CB_1R function, none of them assessed the role of the DRY motif in CB_1R function
130 directly, i.e. through mutational analysis. More importantly, none of the available studies
131 have aimed to identify β-arrestin-regulatory motifs of CB_1R other than the receptor C-

terminus. Therefore, our goal was to analyze the role of the conserved DRY sequence in the G protein activation and β-arrestin binding of CB_1R. We introduced single, double and triple alanine mutations into this site of CB_1R and applied functional assays directly measuring G protein activation, β-arr2 recruitment and intracellular signaling of wild-type and mutant CB_1R variants.

2. Materials and Methods

2.1. Materials

The cDNA of the rat vascular CB_1R was provided by Zsolt Lenkei (Centre National de la Recherche Scientificue, Paris). cDNAs of human β_1 and γ_{11} G protein subunits were purchased from the Missouri S&T cDNA Resource Center (Rolla, MO). β-arr2-eGFP cDNA was kindly provided by Dr. Marc G. Caron (Duke University, Durham, NC). Molecular biology enzymes were obtained from Fermentas (Vilnius, Lithuania) and Stratagene (La Jolla, CA). Fetal bovine serum (FBS), OptiMEM, Lipofectamine 2000, and PBS-EDTA were from Invitrogen (Carlsbad, CA). CHO-K1 and HeLa cell lines were obtained from ATCC (American Type Culture Collection, Manassas, VA). Coelenterazine h was from Regis Technologies (Morton Grove, IL). WIN55,212-2, 2-arachydonoylglycerol and AM251 were from Tocris (Bristol, UK). Cell culture dishes and plates for BRET measurements were from Greiner (Kremsmunster, Austria). Anti-pERK1/2, anti-ERK1/2 and HRP-conjugated anti-rabbit and anti-mouse antibodies were

154 from Cell Signaling Technology Inc. (Beverly, MA). Unless otherwise stated, all other
155 chemicals and reagents were from Sigma (St. Louis, MO).
156
157 *2.2. Plasmid constructs and site-directed mutagenesis*
158
159 The mVenus-tagged rat CB_1R (CB_1R-mVenus) was created by exchanging the sequence
160 of eYFP in CB_1R-eYFP (kindly provided by Zsolt Lenkei (Centre National de la
161 Recherche Scientificue, Paris)) to the sequence of mVenus using AgeI and NotI
162 restriction enzymes. α_o-Rluc and YFP-β_1 constructs were created from α_{oA}-CFP (kindly
163 provided by Dr. N. Gautam (Azpiazu and Gautam 2004)), and β_1, respectively, as
164 described previously (Turu et al. 2007). β-arr2-Rluc was constructed as described
165 previously (Turu et al. 2006). Plasma membrane-targeted mVenus (MP-mVenus) was
166 constructed as described previously (Varnai et al. 2007). Plasma membrane-targeted
167 super Renilla luciferase (MP-Sluc) was generated from MP-mVenus by replacing the
168 mVenus coding sequence with the cDNA of super Renilla luciferase (Woo and von
169 Arnim, 2008).The EPAC-based BRET sensor was constructed as described previously
170 (Erdelyi et al. 2014). Mutations in the DRY motif of CB_1R or CB_1R-mVenus were
171 inserted by the QuikChange® site-directed mutagenesis kit (Stratagene, La Jolla, CA)
172 according to manufacturer's suggestions. Sequences of all constructs were verified using
173 automated DNA sequencing.
174
175 *2.3. Cell culture and transfection*
176

CHO or HeLa cells (passage numbers 5 to 15) were maintained in Ham's F12 or DMEM, respectively, supplemented with 10% FBS, (Invitrogen, Carlsbad, CA), 100 μg/ml streptomycin, and 100 IU/ml penicillin in 5% CO_2 at 37 °C. For confocal microscopy experiments, cells were grown on glass coverslips in 6-well plates and transfected with the indicated constructs using Lipofectamine 2000 in OptiMEM following the manufacturer's instructions. For BRET and Western blot experiments, cells were grown on 6-well plates and transfected with the indicated constructs using Lipofectamine 2000 in OptiMEM following the manufacturer's instructions.

2.4. Bioluminescence resonance energy transfer (BRET) measurements

A detailed description of the BRET measurements applied here can be found in Supplementary Methods.

2.5. Confocal laser-scanning microscopy

Cells were grown on glass coverslips and transfected with the appropriate constructs (using 2 μg/well CB_1R-mVenus or 0.5 μg/well β-arr2-GFP and 2 μg/well CB_1R). Cells were analyzed 22-26 hours later in a modified Krebs-Ringer buffer (see above), using a Zeiss LSM 710 confocal laser scanning microscope.

2.6. Western blot analysis

A detailed description of the Western blot measurements applied here can be found in Supplementary Methods.

2.7. Data analysis

Dose-response curves for G protein, β-arrestin and EPAC BRET measurements were fitted and statistically compared using built-in algorithms of GraphPad Prism 4.03 (GraphPad Software Inc, San Diego, CA). Equimolar comparison was carried out by plotting the points of G protein and β-arr2 BRET dose-response curves for vehicle, -8.0 (only by WIN55), -7.5, -7.0, -6.5, -6.0, -5.5 and -5.0 (only by 2-AG) log[WIN55] or log[2-AG] (M) treatments of the same receptor against each other. Equiactive comparison was carried out by determining the bias factor (β) using the equation $\beta = \log\left(\left(\frac{E_{\max,1}}{EC_{50,1}}\frac{EC_{50,2}}{E_{\max,2}}\right)_{mut} \times \left(\frac{E_{\max,2}}{EC_{50,2}}\frac{EC_{50,1}}{E_{\max,1}}\right)_{ref}\right)$, (Rajagopal et al. 2011), where $E_{max,1}$, $EC_{50,1}$, $E_{max,2}$ and $EC_{50,2}$ are E_{max} and EC_{50} values from G protein and β-arrestin BRET dose-response curves, respectively, using CB_1R-WT as reference receptor. Quantified Western-blot data were evaluated with two-way ANOVA combined with Holm-Sidak's post-hoc test, using the software SigmaStat for Windows 3.5 (Systat Software Inc., Richmond, CA), and a p value <0.05 was considered significant.

3. Results

3.1. Plasma membrane localization of the CB_1R mutants

To investigate whether any of the mutations inserted into the DRY motif of CB_1R affects the proper plasma membrane localization of the receptor, CHO cells expressing mVenus-tagged CB_1R variants were analyzed using confocal microscopy. In resting cells, CB_1R-mVenus is localized both at the plasma membrane and in intracellular vesicles, consistent with the constitutive internalization of CB_1R (Fig. 1A). Importantly, D3.49A mutation strongly impaired plasma membrane localization of CB_1R, with most of the receptors being retained in the endoplasmic reticulum of the cells (CB_1R-D3.49A-mVenus (CB_1R-ARY-mVenus) and CB_1R-D3.49A/Y3.51A-mVenus (CB_1R-ARA-mVenus), Fig. 1B and F, respectively). Interestingly, this effect of the D3.49A mutation was reversed by co-mutation of R3.50, as the double mutant CB_1R-D3.49A/R3.50A (CB_1R-AAY) and the triple mutant CB_1R-D3.49A/R3.50A/Y3.51A (CB_1R-AAA) both showed proper plasma membrane localization (Fig. 1G and H, respectively). The other three mutants, i.e. CB_1R-R3.50A (CB_1R-DAY), CB_1R-Y3.51A (CB_1R-DRA) and CB_1R-R3.50A/Y3.51A (CB_1R-DAA) displayed a cellular distribution roughly similar to that of the wild-type receptor (Fig 1C, D and E, respectively).

Since analysis of confocal images is in many cases not sensitive enough to detect fine changes in receptor distribution, we also applied a more quantifiable approach here, i.e. we measured the BRET interaction levels between CB_1R-mVenus and plasma membrane-targeted Sluc protein. The fraction of the receptors residing on the plasma membrane of non-stimulated cells (PM/total receptor BRET) was found to be similar in cells expressing CB_1R-WT, CB_1R-AAY or CB_1R-AAA, whereas CB_1R-DAY, CB_1R-DRA and CB_1R-DAA showed an ~40% reduction of plasma membrane localization.

245 Furthermore, in accordance with confocal images, the plasma membrane localization of
246 CB_1R-ARY and CB_1R-ARA was shown to be almost completely diminished (Fig. 1I).
247 Since the plasma membrane localization of the CB_1R-ARY and CB_1R-ARA mutants was
248 severely disrupted, these two mutants were not characterized in the subsequent studies.
249
250 *3.2. R3.50A mutation partially affects CB_1R function*
251
252 R3.50 is the most conserved residue within the DRY motif, therefore we first checked the
253 functionality of the CB_1R-DAY mutant. The G protein activation of the receptor was
254 directly monitored by measuring BRET changes between heterotrimeric G_o protein
255 subunits (α_o-Rluc and YFP-$\beta_1\gamma_{11}$) (Turu et al. 2007), co-expressed with wild-type or
256 mutant CB_1R. In control experiments measuring BRET donor and acceptor partner
257 expression directly (i.e. through luminescence and fluorescence counts, respectively) no
258 significant changes were detected between these values when tested with the different
259 CB_1R mutants, suggesting that the observed changes in BRET were not due to alterations
260 in BRET partner stoichiometry. This applies for all of the G_o BRET and β-arrestin BRET
261 experiments presented in this study (data not shown). Dose-response curves performed
262 with the synthetic CB_1R agonist WIN55,212-2 (WIN55) or with the endocannabinoid 2-
263 arachydonoylglycerol (2-AG) showed that the CB_1R-DAY mutant is impaired, but not
264 completely disrupted in its ability to activate G_o proteins. Moreover, CB_1R-DAY shows a
265 basal G protein activation similar to that of CB_1R-WT (Fig. 2A and B). The EC_{50} value of
266 CB_1R-DAY was also similar to that of CB_1R-WT, indicating that the G protein binding of
267 CB_1R is not affected by the R3.50A mutation (Table 1).

Next, the β-arr2 recruitment of CB_1R-DAY was investigated. GFP-tagged β-arr2 (β-arr2-GFP) was co-expressed with CB_1R-DAY in CHO cells, and its distribution was analyzed under confocal microscopy. Interestingly, we found that in cells co-expressing β-arr2-GFP and CB_1R-DAY, β-arr2-GFP was recruited to the plasma membrane in punctuate structures already in resting cells, indicating an increased basal β-arr2 recruitment of CB_1R-DAY (Fig. 2E and G). Such basal recruitment of β-arr2-GFP could not be observed with CB_1R-WT (Fig. 2C). This basal recruitment of β-arr2 was the consequence of a partially active receptor conformation, since treatment with the CB_1R inverse agonist AM251 (10 μM, 10 min) resulted in the disappearance of most of the β-arr2 puncta from the plasma membrane (Fig. 2H).

After addition of the CB_1R agonist WIN55 (1 μM, 10 min) further translocation of β-arr2-GFP to the plasma membrane could be observed in case of CB_1R-DAY, however, this did not reach the level of β-arr2-GFP recruitment of the CB_1R-WT (Fig. 2D and F).

To evaluate β-arr2 recruitment in a more quantitative manner, translocation of β-arr2 to the receptors was followed by monitoring BRET changes between β-arr2-Rluc and plasma membrane targeted mVenus (MP-mVenus). With this assay, β-arr2 recruitment to the investigated receptor can be monitored without tagging the receptor itself directly, which is advantageous because the detected BRET changes are not influenced by possible orientational changes resulting from the introduced receptor mutations. Furthermore, BRET signal in this assay is only affected via receptors residing on the plasma membrane, i.e. BRET ratios are not disturbed by intracellular receptor population. Dose-response curves performed with WIN55 in this β-arr2 BRET assay were in good accordance with the data obtained by confocal microscopy, i.e. the increased basal β-arr2

recruitment of CB_1R-DAY, as well as a lower β-arr2 recruitment in response to agonist stimulus were detectable (Fig. 2I). Similar results were obtained with the endocannabinoid 2-AG (Fig. 2J).

3.3. Y3.51A mutation increases constitutive activity of CB_1R

Among the three residues of the DRY motif, Y3.51 is the least conserved, and relatively little is known about its role in 7TMR signaling. To obtain data about its role in CB_1R regulation, we tested the CB_1R-DRA mutant under our experimental settings. Interestingly, although the maximal G protein activation of this mutant was only marginally impaired (i.e. a significant change in E_{max} was only detectable upon 2-AG stimuli), the G protein BRET dose-response analysis indicated an elevated basal G protein activation for this mutant (Fig. 3A and B, Table 1). Confocal microscopy analysis showed that, similarly to the CB_1R-DAY mutant, basal β-arr2 recruitment of CB_1R-DRA occurs (Fig. 3C and E), which could be reversed by inverse agonist treatment (Fig. 3F). Agonist-induced β-arr2-GFP translocation to the plasma membrane was very weak (Fig. 3D). β-arr2 BRET analysis was in accordance with confocal data, namely, dose-response curve showed elevated basal β-arr2 recruitment together with a significantly impaired agonist-induced β-arr2 translocation (Fig. 3G and H).

3.4. Enhanced β-arrestin2 recruitment and reduced G protein activation of the CB_1R-AAY mutant

Next, we investigated the signaling properties of the double mutant CB_1R-AAY. The G protein activation was monitored by the BRET assay described above. Dose-response curves carried out with WIN55 or 2-AG showed that the CB_1R-AAY mutant has impaired G_o activation ability (Fig. 4A and B), which is reflected both in the E_{max} and the pEC_{50} values of these interactions (Table 1). Moreover, basal G protein activation of this mutant was significantly lowered ((Fig. 4A and B, Table 1).

The β-arr2 recruitment of CB_1R-AAY was investigated also by β-arr2-GFP co-expression under confocal microscope. We found that, similarly to CB_1R-DAY and CB_1R-DRA, CB_1R-AAY recruited β-arr2-GFP to the plasma membrane in non-stimulated cells (Fig. 4C and E). The basal β-arr2 recruitment could be reversed with inverse agonist AM251 treatment (Fig. 4F). Upon addition of WIN55, a very robust translocation of β-arr2-GFP to the plasma membrane was observed, with practically no β-arr2-GFP remaining in the cytoplasm (Fig. 4D). We further evaluated the β-arr2 recruitment of CB_1R-AAY with the BRET-based method described above. WIN55 and 2-AG dose-response curves showed that, in addition to the increased basal β-arr2 recruitment of CB_1R-AAY, this mutant gained a substantially increased ability to recruit β-arr2 upon agonist stimulus, as shown by the significant left- and upward shift of the curves (Fig. 4G and H, Table 1). These results suggest that the signaling of this mutant is shifted from G protein activation towards β-arr2 recruitment, and therefore CB_1R-AAY can be considered as a β-arr2-biased mutant.

The characteristics of the triple mutant CB_1R-AAA) were very similar to that of CB_1R-AAY, i.e. a decrease in basal and agonist-induced G protein activation, as well as an increase in basal and agonist-induced β-arr2 recruitment were observed (data not shown).

337

338 *3.5. The CB_1R-DAA mutant is G protein-biased*

339

340 In the next set of experiments, the functional characteristics of the CB_1R-DAA double
341 mutant receptor were analyzed. Dose-response curves obtained by G_o protein BRET
342 assay showed that the CB_1R-DAA mutant can activate G proteins at a lowered level
343 (~75% of CB_1R-WT), although pEC50 values as well as basal G protein activation
344 remained unaffected (Fig. 5A and B, Table 1).
345 Confocal microscopy analysis of β-arr2-GFP co-expressed with CB_1R-DAA showed that
346 this mutant, similarly to the CB_1R-DAY, CB_1R-DRA and CB_1R-AAY mutants, recruited
347 β-arr2-GFP to the plasma membrane under control conditions (Fig. 5C and E), and this
348 was reversed by AM251 treatment (Fig. 5F). Interestingly, no further translocation of β-
349 arr2-GFP could be detected in these cells upon addition of the CB_1R agonist WIN55 (Fig.
350 5C). These results were strengthened by β-arr2 BRET measurements, showing a basal β-
351 arr2 recruitment for CB_1R-DAA, which, however, cannot be enhanced by WIN55 or 2-
352 AG treatment (Fig. 5G and H). These results suggest that, in contrast to CB_1R-AAY, the
353 signaling of CB_1R-DAA is shifted from β-arr2 recruitment towards G protein activation,
354 and therefore CB_1R-DAA can be considered as a G protein-biased mutant.

355

356 *3.6. β-arrestin1 recruitment of CB_1R-AAY mutant is robustly enhanced*

357

358 In our previous study we could not detect significant β-arr1 coupling to the CB_1R upon
359 WIN55 stimulus, however, others have suggested that CB_1R dependent β-arr1

recruitment can be present and may regulate ERK1/2 activation of CB_1R (Laprairie et al., 2014; Flores-Otero et al., 2014). To test whether DRY mutations of CB_1R affect the recruitment of β-arr1, we applied the same BRET based approach as above, i.e. the plasma membrane translocation of β-arr1-Rluc was monitored, and dose-response curves were performed using WIN55 and 2-AG as agonists. Our results show that agonist-induced β-arr1 recruitment is very low in cells expressing CB_1R-WT, i.e. a significant increase could only be detected upon 2-AG treatment, whereas the changes obtained with WIN55 proved to be non-significant. Interestingly, the CB_1R-AAY mutant displayed a robustly enhanced ability to recruit β-arr1, both upon WIN55 and 2-AG stimuli. All of the other three mutants (i.e. CB_1R-DAY, CB_1R-DRA and CB_1R-DAA) produced non-significant changes in the plasma membrane localization of β-arr1 (Fig. 6A and B).

3.7. Detailed data analysis strengthens biased signaling of DRY mutant CB_1Rs

The above results suggest that distinct mutations in the conserved DRY motif of the CB_1R can differentially affect G protein activation and β-arr2 recruitment of the receptor. To assess this receptor bias in an exact manner, two different methods, proposed by Rajagopal et al. (Rajagopal et al. 2011), were applied to analyze data. First, 'equimolar comparison' was carried out, where G protein and β-arr2 responses elicited by the same ligand concentrations are plotted against each other. In the case of the 'reference receptor', i.e. CB_1R-WT, this analysis yields a roughly hyperbolic shape with both WIN55 and 2-AG (Fig. 7A and B, respectively, black circles), reflecting the difference in the amplification between G protein and β-arr2 assays. Importantly, the points for CB_1R-

AAY are substantially shifted left- and upwards on these graphs, representing bias towards β-arr2 recruitment (Fig. 7A and B, white triangles). Furthermore, the points for CB_1R-DAA are arranged along a horizontal line, demonstrating the bias of this receptor towards G protein activation (Fig. 7A and B, grey squares). The other method was 'equiactive comparison', where the signaling of each receptor is characterized by a bias factor (β), based on the EC_{50} and E_{max} values from G protein and β-arr2 dose-response curves (Rajagopal et al. 2011). In case of the reference receptor (CB_1R-WT), this bias factor is by definition 0. In the case of CB_1R-DAA, the β values were 1.42 or 1.61 (for WIN55 or 2-AG stimuli, respectively), whereas the same values for CB_1R-AAY were -1.54 or -1.42, representing more than 10-fold bias of these two mutants towards G protein activation and β-arr2 recruitment, respectively (Fig. 7C).

Taken together, our detailed bias analysis indicated that CB_1R-AAY and CB_1R-DAA can be considered as β-arrestin-biased and G protein-biased mutants, respectively.

3.8. Functional assays reflect biased intracellular signaling of CB_1R-AAY and CB_1R-DAA

Next, we wanted to assess whether the differences seen at the level of receptor-effector protein coupling are reflected in more distal intracellular signaling events initiated by CB_1R activation. First, $G_{i/o}$ protein-mediated signaling was assessed by measuring inhibition of forskolin-induced cAMP accumulation under basal and CB_1R-stimulated conditions, using an EPAC-based intramolecular BRET-sensor (Erdelyi et al. 2014). Our results showed that CB_1R-WT inhibits cAMP accumulation under non-stimulated

conditions, and this is substantially and dose-dependently enhanced upon treatment with WIN55 (Fig. 8A). Importantly, WIN55-induced cAMP inhibition of the G protein-biased mutant CB_1R-DAA was lower but still present, whereas CB_1R-AAY, in accordance with its bias towards β-arr2, failed to induce the inhibition of cAMP accumulation in response to agonist stimulus (Fig. 8A).

Recent data suggest that CB_1R-induced p42/44 MAP kinase (ERK1/2) activation, which was formerly suggested to occur via G protein-dependent pathways (Galve-Roperh et al. 2002; Davis et al. 2003; Dalton and Howlett 2012), is also mediated by β-arrestins (Ahn et al. 2013a; Mahavadi et al. 2014). Therefore, we aimed to study how the ERK1/2 responses correlate with the G protein activation and/or β-arrestin recruitment of the biased CB_1R mutants. Western blot experiments carried out with cells expressing CB_1R-WT showed a robust increase in the amount of phosphorylated ERK1/2 (pERK1/2) after 5 min treatment with WIN55 (1 μM). Moreover, lower but sustained pERK1/2 levels were also detectable after 20 min WIN55 treatment (Fig. 7B and C). Interestingly, we found that the β-arr2-biased CB_1R-AAY elicited pERK1/2 responses similar to CB_1R-WT, both at 5 and 20 min stimulation, whereas the G protein-biased CB_1R-DAA produced significantly lower pERK1/2 responses than the wild-type receptor (Fig. 7B and C). Thus, ERK1/2 activation of the biased DRY mutants correlated well with their β-arr2 recruitment ability, rather than with their G protein activation.

4. Discussion

In this study, we evaluated the role of the conserved DRY motif in the function of the CB_1R. Our goal was to assess its role in mediating basal and agonist-induced G protein activation and β-arrestin recruitment of CB_1R, as well as to identify possible differences caused in these two main effector functions of the receptor. Interestingly, single alanine mutation of the conserved Arg (R3.50A) resulted only in a ~20% reduction of the G protein coupling efficiency of CB_1R, without affecting its basal G protein activation. This may seem surprising, as crystal structure analysis as well as several mutational data have suggested a pivotal role for this residue in the G protein coupling of 7TMRs (Zhu et al. 1994; Ballesteros et al. 1998; Rasmussen et al. 2011). However, several other 7TMRs exist, where similar non-conservative mutations of R3.50 failed to abolish G protein activation of the receptor (Fanelli et al. 1999; Rovati et al. 2007). Thus, CB_1R appears to belong to a subgroup of 7TMRs where this conserved Arg residue plays no absolute role in the direct receptor-G protein coupling. Furthermore, our results demonstrate a basal β-arr2 recruitment of the CB_1R-DAY mutant (or any double or triple mutant carrying the same mutation), which is in good accordance with previously published data showing similar characteristics for R3.50H mutants of V_2 vasopressin, α_{1B} adrenergic and AT_{1A} angiotensin II receptors (Wilbanks et al. 2002). This strengthens the idea that this conserved Arg somehow prevents arrestin binding in the inactive receptor conformation. Agonist-induced β-arr2 recruitment of CB_1R-DAY and CB_1R-DRA was lowered, which is most likely to be caused by the lowered plasma membrane localization of these mutants (Fig. 1I).

The most interesting finding of our study is the major difference between the functions of two double mutants, CB_1R-DAA and CB_1R-AAY. Although both mutants contain the

451 R3.50A mutation, and accordingly show increased basal β-arr2 recruitment, their ultimate
452 characteristics are further determined by the location of the second mutation. Thereby, a
453 simultaneous lack of D3.49 and R3.50 residues seems to have a dominant-positive effect
454 on both the β-arr1 and β-arr2 recruitment of CB_1R (which is also supported by the fact
455 that the triple mutant CB_1R-AAA functionally resembles CB_1R-AAY). Thus, CB_1R-AAY
456 is a β-arrestin-biased 7TMR mutant. Interestingly, these characteristics of the CB_1R-AAY
457 are similar to those of the formerly described biased mutant angiotensin II receptor AT_1-
458 DRY/AAY (AT_1R-AAY) (Gaborik et al. 2003; Wei et al. 2003). However, an important
459 difference here is that AT_1R-AAY is β-arrestin-biased in a way that its G protein
460 activation is absent while its β-arrestin binding is present but certainly not increased (Wei
461 et al. 2003, Balla et al., 2012), whereas CB_1R-AAY is β-arrestin-biased in that its β-
462 arrestin recruitment is substantially increased, together with a lowered, but not abolished
463 G protein activating ability. Furthermore, we were able to detect a robustly enhanced β-
464 arr1 recruitment to CB_1R-AAY, whereas β-arr1 translocation to CB_1R-WT was
465 significant only upon 2-AG stimulus, but not after WIN55 treatment. Thus, it appears that
466 the recruitment of β-arr1 to CB_1R-WT is very weak, so that it challenges the limits of
467 detectability via the (otherwise quite sensitive) BRET approach applied here. However,
468 our results showing a significant increase of β-arr1 BRET upon 2-AG stimulus are in
469 accordance with recent results showing higher β-arr1 recruitment by 2-AG compared to
470 WIN55 (Laprairie et al., 2014). Taken together, recruitment of β-arr1 to CB_1R-WT is
471 obviously lower than that of β-arr2, but both are substantially enhanced in the CB_1R-
472 AAY mutant. Interestingly, basal G protein activation of CB_1R-AAY was absent, while
473 the difference between vehicle-treated and WIN55-stimulated cells remained comparable

474 to that of CB_1R-WT (Fig. 4A), raising the question whether the reduced E_{max} value of
475 CB_1R-AAY in this assay reflects a true loss of agonist-induced G protein activation, or it
476 is caused merely by the absence of basal activity, while WIN55-induced G protein
477 activation remains unaffected. However, repeating these experiments in HeLa cells,
478 where basal activity of CB_1R is minimal (Gyombolai et al. 2013), also showed
479 substantially impaired WIN55-induced G protein activation of CB_1R-AAY (Suppl. Fig.
480 1), suggesting that this mutation reduces not only the basal but also the WIN55-induced
481 G_o protein activation of CB_1R.
482 In contrast, CB_1R-DAA proved to be G protein-biased, as its β-arrestin recruitment in
483 response to agonist stimulus was practically absent, but was still able to activate G
484 proteins, although at a lower level (~70% of the wild type CB_1R). According to our data,
485 plasma membrane expression of this mutant is ~40% lower than that of CB_1R-WT.
486 However, this extent of decrease is not likely to cause a complete loss of agonist-induced
487 β-arrestin recruitment, given the ~1:1 stoichiometry of receptor-β-arrestin complex. This
488 is also supported by the fact that CB_1R-DAA still binds β-arr2 under basal conditions.
489 Other 7TMRs described previously as biased mutants include the M_3-R3.50L designer
490 muscarinic receptor (Nakajima and Wess 2012) and β_2-AR-TYY, a triple mutant β_2-AR
491 which was rationally designed to be functionally selective (Shenoy et al. 2006).
492 Interestingly, however, all of these mutants are β-arrestin-biased, i.e. they do not couple
493 to G proteins but still recruit β-arrestin, albeit at a lowered level. The CB_1R-DAA mutant
494 presented here is interesting in this respect, as it is biased towards G protein activation,
495 whereas its mutations affect a ‘classical’ G protein-coupling region, i.e. the DRY motif.
496 Intriguingly, although CB_1R-DAA can hardly recruit β-arrestins in response to agonist

497 stimulus, it still binds β-arr2 to some extent under non-stimulated conditions. This relies
498 most probably on the presence of the R3.50A mutation, because, as mentioned above, all
499 of the CB_1R mutants carrying this mutation recruited β-arr2 constitutively. Thus, it seems
500 that the absence of the conserved Arg residue can itself determine a receptor
501 conformation that binds β-arrestin spontaneously. On the other hand, the agonist-induced
502 β-arr2 binding of the receptor can still be strongly influenced in both directions by co-
503 mutations of the neighboring residues.
504 Taken together, our results obtained with the CB_1R-AAY and CB_1R-DAA mutants
505 strongly support a model where the active G protein-coupled and β-arrestin-bound
506 conformations of a 7TMR are different. Moreover, receptor states responsible for
507 constitutive and agonist-induced β-arrestin binding may also show differences.
508 We also demonstrate here that the agonist-induced ERK1/2 phosphorylation shows good
509 correlation with the β-arr2 recruitment of our biased CB_1R mutants, rather than their G
510 protein activation or their ability to inhibit forskolin-induced cAMP accumulation. These
511 data are consistent with the recently emerging concept of β-arrestin-dependent CB_1R
512 signaling, i.e. a β-arrestin-mediated ERK1/2 phosphorylation following CB_1R activation
513 (Ahn et al. 2013a; Mahavadi et al. 2014).
514 One of the most interesting questions regarding the DRY mutants presented here is how
515 (i.e. through which molecular structural rearrangements) the distinct mutations induce
516 such large differences in the β-arrestin-recruitment of CB_1R. One simple explanation
517 would be that mutations of the DRY motif modify primarily the G protein binding of the
518 receptor, and their effects on the β-arr2 recruitment are merely secondary, resulting from
519 the assumption that G proteins and β-arrestins compete for the 7TMR binding. However,

520 if this would be the only explanation, one should observe an indirect proportionality
521 between the G protein-and the β-arrestin binding abilities of the distinct mutants, which is
522 actually not the case. Thus, mutations of the DRY motif most probably affect β-arr2
523 binding of CB_1R independently of its G protein activation. Whether or not the DRY
524 sequence itself is a part of the docking site for arrestins, can not be answered
525 unequivocally based on our results. However, previously published data indicating that
526 the ICL2 loop of 7TMRs, beginning with an intact DRY motif, is part of the β-arrestin
527 binding site, add interesting aspects to our study (Huttenrauch et al. 2002; Marion et al.
528 2006). Moreover, two recent studies have provided important insights into the structural
529 features within the 7TMR-β-arrestin complex. Both of these studies point to an important
530 interaction between the 'finger loop' region of β-arrestin and the receptor core, with the
531 direct involvement of the DRY motif (Shukla et al., 2014; Szczepek et al., 2014).
532 Combined with these data, our results show good fit with a model where DRY is directly
533 involved in the β-arrestin binding of CB_1R. Additionally, mutations of the DRY motif
534 may also affect β-arrestin binding indirectly, i.e. by inducing structural rearrangements in
535 the subsequent ICL2, resulting in diverse, sometimes completely opposite β-arrestin
536 binding phenotypes. However, a more precise understanding of the intramolecular
537 interactions that mediate these characteristics would require the high resolution crystal
538 structure data.
539
540 **Declaration of interest**
541 The authors declare no conflict of interest.
542

Funding

This research was supported by Hungarian Scientific Research Fund (OTKA NK-100883), and a Marie Curie International Outgoing Fellowship within the 7th European Community Framework Programme (PIOF-GA-2009-253628).

Author contributions

P.G. designed and carried out most of the experiments and wrote the manuscript. A.D.T. carried out the β-arr2 BRET experiments, helped with data evaluation and revised the manuscript. D.T. created the CB_1R-DAY mutant and carried out important control experiments. G.T. created the CB_1R-AAY mutant, helped with data interpretation and revised the manuscript. L.H. managed the overall project, helped with data interpretation and revised the manuscript.

Acknowledgements

The excellent technical assistance of Ilona Oláh, as well as the help of Bence Szalai with the statistical analyses and presentation of the data is greatly appreciated.

References

Ahn, KH, Mahmoud, MM, Shim, JY & Kendall, DA 2013a Distinct roles of beta-arrestin 1 and beta-arrestin 2 in ORG27569-induced biased signaling and internalization of the cannabinoid receptor 1 (CB1). *The Journal of Biological Chemistry* **288** 9790-9800

566 Ahn, KH, Scott, CE, Abrol, R, Goddard, WA, III & Kendall, DA 2013b
567 Computationally-predicted CB1 cannabinoid receptor mutants show distinct
568 patterns of salt-bridges that correlate with their level of constitutive activity
569 reflected in G protein coupling levels, thermal stability, and ligand binding.
570 *Proteins* **81** 1304-1317

571 Azpiazu, I & Gautam, N 2004 A fluorescence resonance energy transfer-based sensor
572 indicates that receptor access to a G protein is unrestricted in a living mammalian
573 cell. *The Journal of Biological Chemistry* **279** 27709-27718

574 Balla, A, Toth, DJ, Soltesz-Katona, E, Szakadati, G, Erdelyi, LS, Varnai, P & Hunyady,
575 L 2012 Mapping of the localization of type 1 angiotensin receptor in membrane
576 microdomains using bioluminescence resonance energy transfer-based sensors. *J.*
577 *Biol. Chem.* **287** 9090-9099

578 Ballesteros, J, Kitanovic, S, Guarnieri, F, Davies, P, Fromme, BJ, Konvicka, K, Chi, L,
579 Millar, RP, Davidson, JS, Weinstein, H & Sealfon, SC 1998 Functional
580 microdomains in G-protein-coupled receptors. The conserved arginine-cage motif
581 in the gonadotropin-releasing hormone receptor. *The Journal of Biological*
582 *Chemistry* **273** 10445-10453

583 Ballesteros, JA, Jensen, AD, Liapakis, G, Rasmussen, SG, Shi, L, Gether, U & Javitch,
584 JA 2001 Activation of the beta 2-adrenergic receptor involves disruption of an
585 ionic lock between the cytoplasmic ends of transmembrane segments 3 and 6. *The*
586 *Journal of Biological Chemistry* **276** 29171-29177

587 Barak, LS, Oakley, RH, Laporte, SA & Caron, MG 2001 Constitutive arrestin-mediated
588 desensitization of a human vasopressin receptor mutant associated with
589 nephrogenic diabetes insipidus. *Proceedings of the National Academy of Sciences*
590 *of the United States of America* **98** 93-98

591 Daigle, TL, Kwok, ML & Mackie, K 2008 Regulation of CB1 cannabinoid receptor
592 internalization by a promiscuous phosphorylation-dependent mechanism. *Journal*
593 *of Neurochemistry* **106** 70-82

594 Dalton, GD & Howlett, AC 2012 Cannabinoid CB1 receptors transactivate multiple
595 receptor tyrosine kinases and regulate serine/threonine kinases to activate ERK in
596 neuronal cells. *British Journal of Pharmacology* **165** 2497-2511

597 Davis, MI, Ronesi, J & Lovinger, DM 2003 A predominant role for inhibition of the
598 adenylate cyclase/protein kinase A pathway in ERK activation by cannabinoid
599 receptor 1 in N1E-115 neuroblastoma cells. *The Journal of Biological Chemistry*
600 **278** 48973-48980

601 DeWire, SM, Ahn, S, Lefkowitz, RJ & Shenoy, SK 2007 Beta-arrestins and cell
602 signaling. *Annual Review of Physiology* **69** 483-510

603 Erdelyi, LS, Balla, A, Patocs, A, Toth, M, Varnai, P & Hunyady, L 2014 Altered agonist
604 sensitivity of a mutant v2 receptor suggests a novel therapeutic strategy for
605 nephrogenic diabetes insipidus. *Molecular Endocrinology* **28** 634-643

606 Fanelli, F, Barbier, P, Zanchetta, D, de Benedetti, PG & Chini, B 1999 Activation
607 mechanism of human oxytocin receptor: a combined study of experimental and
608 computer-simulated mutagenesis. *Molecular Pharmacology* **56** 214-225

609 Flores-Otero, J, Ahn, KH, Delgado-Peraza, F, Mackie, K, Kendall, DA & Yudowski, GA
610 2014 Ligand-specific endocytic dwell times control functional selectivity of the
611 cannabinoid receptor 1. *Nat. Commun.* **5** 4589

612 Gaborik, Z, Jagadeesh, G, Zhang, M, Spat, A, Catt, KJ & Hunyady, L 2003 The role of a
613 conserved region of the second intracellular loop in AT1 angiotensin receptor
614 activation and signaling. *Endocrinology* **144** 2220-2228

615 Galve-Roperh, I, Rueda, D, Gomez del Pulgar, T, Velasco, G & Guzman, M 2002
616 Mechanism of extracellular signal-regulated kinase activation by the CB(1)
617 cannabinoid receptor. *Molecular Pharmacology* **62** 1385-1392

618 Glass, M & Northup, JK 1999 Agonist selective regulation of G proteins by cannabinoid
619 CB(1) and CB(2) receptors. *Molecular Pharmacology* **56** 1362-1369

620 Gurevich, VV & Benovic, JL 1993 Visual arrestin interaction with rhodopsin. Sequential
621 multisite binding ensures strict selectivity toward light-activated phosphorylated
622 rhodopsin. *The Journal of Biological Chemistry* **268** 11628-11638

623 Gurevich, VV & Gurevich, EV 2006 The structural basis of arrestin-mediated regulation
624 of G-protein-coupled receptors. *Pharmacology & Therapeutics* **110** 465-502

625 Gyombolai, P, Boros, E, Hunyady, L & Turu, G 2013 Differential beta-arrestin2
626 requirements for constitutive and agonist-induced internalization of the CB1
627 cannabinoid receptor. *Molecular and Cellular Endocrinology* **372** 116-127

628 Huttenrauch, F, Nitzki, A, Lin, FT, Honing, S & Oppermann, M 2002 Beta-arrestin
629 binding to CC chemokine receptor 5 requires multiple C-terminal receptor
630 phosphorylation sites and involves a conserved Asp-Arg-Tyr sequence motif. *The*
631 *Journal of Biological Chemistry* **277** 30769-30777

632 Kim, KM & Caron, MG 2008 Complementary roles of the DRY motif and C-terminus
633 tail of GPCRS for G protein coupling and beta-arrestin interaction. *Biochemical*
634 *and Biophysical Research Communications* **366** 42-47

635 Kouznetsova, M, Kelley, B, Shen, M & Thayer, SA 2002 Desensitization of cannabinoid-
636 mediated presynaptic inhibition of neurotransmission between rat hippocampal
637 neurons in culture. *Molecular Pharmacology* **61** 477-485

638 Laprairie, RB, Bagher, AM, Kelly, ME, Dupre, DJ & Denovan-Wright, EM 2014 Type 1
639 cannabinoid receptor ligands display functional selectivity in a cell culture model
640 of striatal medium spiny projection neurons. *J. Biol. Chem.* **289** 24845-24862

641 Leterrier, C, Laine, J, Darmon, M, Boudin, H, Rossier, J & Lenkei, Z 2006 Constitutive
642 activation drives compartment-selective endocytosis and axonal targeting of type
643 1 cannabinoid receptors. *The Journal of Neuroscience : the Official Journal of the*
644 *Society for Neuroscience* **26** 3141-3153

Li, J, Huang, P, Chen, C, de Riel, JK, Weinstein, H & Liu-Chen, LY 2001 Constitutive activation of the mu opioid receptor by mutation of D3.49(164), but not D3.32(147): D3.49(164) is critical for stabilization of the inactive form of the receptor and for its expression. *Biochemistry* **40** 12039-12050

Mahavadi, S, Sriwai, W, Huang, J, Grider, JR & Murthy, KS 2014 Inhibitory signaling by CB1 receptors in smooth muscle mediated by GRK5/beta-arrestin activation of ERK1/2 and Src kinase. *American Journal of Physiology. Gastrointestinal and Liver Physiology* **306** G535-G545

Marion, S, Oakley, RH, Kim, KM, Caron, MG & Barak, LS 2006 A beta-arrestin binding determinant common to the second intracellular loops of rhodopsin family G protein-coupled receptors. *The Journal of Biological Chemistry* **281** 2932-2938

McDonald, NA, Henstridge, CM, Connolly, CN & Irving, AJ 2007 An essential role for constitutive endocytosis, but not activity, in the axonal targeting of the CB1 cannabinoid receptor. *Molecular Pharmacology* **71** 976-984

Mukhopadhyay, S & Howlett, AC 2001 CB1 receptor-G protein association. Subtype selectivity is determined by distinct intracellular domains. *European Journal of Biochemistry / FEBS* **268** 499-505

Nakajima, K & Wess, J 2012 Design and functional characterization of a novel, arrestin-biased designer G protein-coupled receptor. *Molecular Pharmacology* **82** 575-582

Pacher, P, Batkai, S & Kunos, G 2006 The endocannabinoid system as an emerging target of pharmacotherapy. *Pharmacological Reviews* **58** 389-462

666 Rajagopal, S, Ahn, S, Rominger, DH, Gowen-MacDonald, W, Lam, CM, DeWire, SM,
667 Violin, JD & Lefkowitz, RJ 2011 Quantifying ligand bias at seven-
668 transmembrane receptors. *Molecular Pharmacology* **80** 367-377

669 Rasmussen, SG, DeVree, BT, Zou, Y, Kruse, AC, Chung, KY, Kobilka, TS, Thian, FS,
670 Chae, PS, Pardon, E, Calinski, D, Mathiesen, JM, Shah, ST, Lyons, JA, Caffrey,
671 M, Gellman, SH, Steyaert, J, Skiniotis, G, Weis, WI, Sunahara, RK & Kobilka,
672 BK 2011 Crystal structure of the beta2 adrenergic receptor-Gs protein complex.
673 *Nature* **477** 549-555

674 Reiter, E, Ahn, S, Shukla, AK & Lefkowitz, RJ 2012 Molecular mechanism of beta-
675 arrestin-biased agonism at seven-transmembrane receptors. *Annual Review of*
676 *Pharmacology and Toxicology* **52** 179-197

677 Rhee, MH, Nevo, I, Levy, R & Vogel, Z 2000 Role of the highly conserved Asp-Arg-Tyr
678 motif in signal transduction of the CB2 cannabinoid receptor. *FEBS Letters* **466**
679 300-304

680 Rovati, GE, Capra, V & Neubig, RR 2007 The highly conserved DRY motif of class A G
681 protein-coupled receptors: beyond the ground state. *Molecular Pharmacology* **71**
682 959-964

683 Scheer, A, Fanelli, F, Costa, T, de Benedetti, PG & Cotecchia, S 1996 Constitutively
684 active mutants of the alpha 1B-adrenergic receptor: role of highly conserved polar
685 amino acids in receptor activation. *The EMBO Journal* **15** 3566-3578

686 Scheer, A, Fanelli, F, Costa, T, de Benedetti, PG & Cotecchia, S 1997 The activation
687 process of the alpha1B-adrenergic receptor: potential role of protonation and
688 hydrophobicity of a highly conserved aspartate. *Proceedings of the National*
689 *Academy of Sciences of the United States of America* **94** 808-813

690 Scott, CE, Abrol, R, Ahn, KH, Kendall, DA & Goddard, WA, III 2013 Molecular basis
691 for dramatic changes in cannabinoid CB1 G protein-coupled receptor activation
692 upon single and double point mutations. *Protein Science : a Publication of the*
693 *Protein Society* **22** 101-113

694 Shenoy, SK, Drake, MT, Nelson, CD, Houtz, DA, Xiao, K, Madabushi, S, Reiter, E,
695 Premont, RT, Lichtarge, O & Lefkowitz, RJ 2006 beta-arrestin-dependent, G
696 protein-independent ERK1/2 activation by the beta2 adrenergic receptor. *The*
697 *Journal of Biological Chemistry* **281** 1261-1273

698 Shenoy, SK & Lefkowitz, RJ 2011 beta-Arrestin-mediated receptor trafficking and signal
699 transduction. *Trends in Pharmacological Sciences* **32** 521-533

700 Shim, JY, Ahn, KH & Kendall, DA 2013 Molecular basis of cannabinoid CB1 receptor
701 coupling to the G protein heterotrimer Galphaibetagamma: identification of key
702 CB1 contacts with the C-terminal helix alpha5 of Galphai. *The Journal of*
703 *Biological Chemistry* **288** 32449-32465

704 Shukla, AK, Westfield, GH, Xiao, K, Reis, RI, Huang, LY, Tripathi-Shukla, P, Qian, J,
705 Li, S, Blanc, A, Oleskie, AN, Dosey, AM, Su, M, Liang, CR, Gu, LL, Shan, JM,
706 Chen, X, Hanna, R, Choi, M, Yao, XJ, Klink, BU, Kahsai, AW, Sidhu, SS, Koide,

S, Penczek, PA, Kossiakoff, AA, Woods, VL, Jr., Kobilka, BK, Skiniotis, G & Lefkowitz, RJ 2014 Visualization of arrestin recruitment by a G-protein-coupled receptor. *Nature* **512** 218-222

Szczepek, M, Beyriere, F, Hofmann, KP, Elgeti, M, Kazmin, R, Rose, A, Bartl, FJ, von Stetten, D, Heck, M, Sommer, ME, Hildebrand, PW & Scheerer, P 2014 Crystal structure of a common GPCR-binding interface for G protein and arrestin. *Nat. Commun.* **5** 4801

Turu, G & Hunyady, L 2010 Signal transduction of the CB1 cannabinoid receptor. *Journal of Molecular Endocrinology* **44** 75-85

Turu, G, Simon, A, Gyombolai, P, Szidonya, L, Bagdy, G, Lenkei, Z & Hunyady, L 2007 The role of diacylglycerol lipase in constitutive and angiotensin AT1 receptor-stimulated cannabinoid CB1 receptor activity. *The Journal of Biological Chemistry* **282** 7753-7757

Turu, G, Szidonya, L, Gaborik, Z, Buday, L, Spat, A, Clark, AJ & Hunyady, L 2006 Differential beta-arrestin binding of AT1 and AT2 angiotensin receptors. *FEBS Letters* **580** 41-45

Varnai, P, Toth, B, Toth, DJ, Hunyady, L & Balla, T 2007 Visualization and manipulation of plasma membrane-endoplasmic reticulum contact sites indicates the presence of additional molecular components within the STIM1-Orai1 Complex. *The Journal of Biological Chemistry* **282** 29678-29690

727 Venkatakrishnan, AJ, Deupi, X, Lebon, G, Tate, CG, Schertler, GF & Babu, MM 2013
728 Molecular signatures of G-protein-coupled receptors. *Nature* **494** 185-194

729 Wei, H, Ahn, S, Shenoy, SK, Karnik, SS, Hunyady, L, Luttrell, LM & Lefkowitz, RJ
730 2003 Independent beta-arrestin 2 and G protein-mediated pathways for
731 angiotensin II activation of extracellular signal-regulated kinases 1 and 2.
732 *Proceedings of the National Academy of Sciences of the United States of America*
733 **100** 10782-10787

734 Wilbanks, AM, Laporte, SA, Bohn, LM, Barak, LS & Caron, MG 2002 Apparent loss-of-
735 function mutant GPCRs revealed as constitutively desensitized receptors.
736 *Biochemistry* **41** 11981-11989

737 Woo, J & von Arnim, AG 2008 Mutational optimization of the coelenterazine-dependent
738 luciferase from Renilla. *Plant Methods* **4** 23

739 Zhu, SZ, Wang, SZ, Hu, J & el Fakahany, EE 1994 An arginine residue conserved in
740 most G protein-coupled receptors is essential for the function of the m1
741 muscarinic receptor. *Molecular Pharmacology* **45** 517-523

742

743

744

745 **Figure legends**

746

747 **Fig.1 Cellular distribution of wild-type and mutant mVenus-tagged CB_1R variants**

748 A-H, CHO cells expressing mVenus-tagged CB_1R variants are visualized using confocal
749 microscopy. A, CB_1R-WT-mVenus B, CB_1R-ARY-mVenus C, CB_1R-DAY-mVenus, D,
750 CB_1R-DRA-mVenus E, CB_1R-DAA-mVenus F, CB_1R-ARA-mVenus G, CB_1R-AAY-
751 mVenus H, CB_1R-AAA-mVenus. Images are representative from 3 independent
752 experiments. Scale bar 10 μm. I, PM/total receptor BRET showing the fraction of
753 mVenus-tagged CB_1R variants residing on the plasma membrane. 0% reflects no net
754 BRET interaction and 100% reflects normalized BRET interaction of CB_1R-WT-
755 mVenus. Data are mean±SEM, n=3, *$p<0.05$, ns – non-significant

756

757 **Fig.2 Functional analysis of the CB_1R-DAY mutant**

758 A-B, Dose-response curves showing G protein activation of CB_1R-WT (grey curve) and
759 CB_1R-DAY (black curve) in CHO cells under basal and different WIN55- (A) or 2-AG-
760 (B) stimulated conditions, as detected by G_o protein BRET. 0% reflects total inactivity of
761 receptors, achieved by inverse agonist treatment (AM251, 10 μM), and 100% reflects
762 maximal WIN55- (A) or 2-AG- (B) induced response (E_{max}) of CB_1R-WT. Data are
763 mean±SEM, n=3-8.

764 C-H, Confocal images showing distribution of β-arr2-GFP in CHO cells co-expressing
765 CB_1R-WT (C and D) or CB_1R-DAY (E-H), under control conditions (C, E and G) and 10
766 min after WIN55 (1 μM, D and F) or AM251 (10 μM, H) treatment. Arrows indicate β-

767 arr2-GFP puncta at the plasma membrane. Images are representative from at least 4
768 independent experiments. Scale bar 10 μm.
769 I-J, Dose-response curves showing recruitment of β-arr2 to the plasma membrane by
770 CB_1R-WT (grey curve) and CB_1R-DAY (black curve) in CHO cells under basal and
771 different WIN55- (I) or 2-AG- (J) stimulated conditions, as detected by BRET between β-
772 arr2-Rluc and MP-mVenus. 0% reflects total inactivity of receptors, achieved by inverse
773 agonist treatment (AM251, 10 μM), and 100% reflects maximal WIN55- (I) or 2-AG- (J)
774 induced response (E_{max}) of CB_1R-WT. Data are mean±SEM, n=4-7.
775
776 **Fig.3 Functional analysis of the CB_1R-DRA mutant**
777 A-B, Dose-response curves showing G protein activation of CB_1R-WT (grey curve) and
778 CB_1R-DRA (black curve) in CHO cells under basal and different WIN55- (A) or 2-AG-
779 (B) stimulated conditions, as detected by G_o protein BRET. 0% reflects total inactivity of
780 receptors, achieved by inverse agonist treatment (AM251, 10 μM), and 100% reflects
781 maximal WIN55- (A) or 2-AG- (B) induced response (E_{max}) of CB_1R-WT. Data are
782 mean±SEM, n=4-8.
783 C-F, Confocal images showing distribution of β-arr2-GFP in CHO cells co-expressing
784 CB_1R-DRA, under control conditions (C and E) and 10 min after WIN55 (1 μM, D) or
785 AM251 (10 μM, F) treatment. Arrows indicate β-arr2-GFP puncta at the plasma
786 membrane. Images are representative from at least 4 independent experiments. Scale bar
787 10 μm.
788 G-H, Dose-response curves showing recruitment of β-arr2 to the plasma membrane by
789 CB_1R-WT (grey curve) and CB_1R-DRA (black curve) in CHO cells under basal and

790 different WIN55- (G) or 2-AG- (H) stimulated conditions, as detected by BRET between
791 β-arr2-Rluc and MP-mVenus. 0% reflects total inactivity of receptors, achieved by
792 inverse agonist treatment (AM251, 10 μM), and 100% reflects maximal WIN55- (G) or
793 2-AG- (H) induced response (E_{max}) of CB_1R-WT. Data are mean±SEM, n=4-7.
794
795 **Fig.4 Functional analysis of the CB_1R-AAY mutant**
796 A-B, Dose-response curves showing G protein activation of CB_1R-WT (grey curve) and
797 CB_1R-AAY (black curve) in CHO cells under basal and different WIN55- (A) or 2-AG-
798 (B) stimulated conditions, as detected by G_o protein BRET. 0% reflects total inactivity of
799 receptors, achieved by inverse agonist treatment (AM251, 10 μM), and 100% reflects
800 maximal WIN55- (A) or 2-AG- (B) induced response (E_{max}) of CB_1R-WT. Data are
801 mean±SEM, n=3-8.
802 C-F, Confocal images showing distribution of β-arr2-GFP in CHO cells co-expressing
803 CB_1R-AAY, under control conditions (C and E) and 10 min after WIN55 (1 μM, D) or
804 AM251 (10 μM, F) treatment. Images are representative from at least 3 independent
805 experiments. Scale bar 10 μm.
806 G-H, Dose-response curves showing recruitment of β-arr2 to the plasma membrane by
807 CB_1R-WT (grey curve) and CB_1R-AAY (black curve) in CHO cells under basal and
808 different WIN55- (G) or 2-AG- (H) stimulated conditions, as detected by BRET between
809 β-arr2-Rluc and MP-mVenus. 0% reflects total inactivity of receptors, achieved by
810 inverse agonist treatment (AM251, 10 μM), and 100% reflects maximal WIN55- (G) or
811 2-AG- (H) induced response (E_{max}) of CB_1R-WT. Data are mean±SEM, n=4-7.
812

Fig.5 Functional analysis of the CB_1R-DAA mutant

A-B, Dose-response curves showing G protein activation of CB_1R-WT (grey curve) and CB_1R-DAA (black curve) in CHO cells under basal and different WIN55- (A) or 2-AG- (B) stimulated conditions, as detected by G_o protein BRET. 0% reflects total inactivity of receptors, achieved by inverse agonist treatment (AM251, 10 μM), and 100% reflects maximal WIN55- (A) or 2-AG- (B) induced response (E_{max}) of CB_1R-WT. Data are mean±SEM, n=4-8.

C-F, Confocal images showing distribution of β-arr2-GFP in CHO cells co-expressing CB_1R-DAA, under control conditions (C and E) and 10 min after WIN55 (1 μM, D) or AM251 (10 μM, F) treatment. Images are representative from at least 3 independent experiments. Scale bar 10 μm.

G-H, Dose-response curves showing recruitment of β-arr2 to the plasma membrane by CB_1R-WT (grey curve) and CB_1R-DAA (black triangles) in CHO cells under basal and different WIN55- (G) or 2-AG- (H) stimulated conditions, as detected by BRET between β-arr2-Rluc and MP-mVenus. 0% reflects total inactivity of receptors, achieved by inverse agonist treatment (AM251, 10 μM), and 100% reflects maximal WIN55- (G) or 2-AG- (H) induced response (E_{max}) of CB_1R-WT. Data are mean±SEM, n=4-7.

Fig.6 Dose-response curves showing β-arrestin1 recruitment of CB_1R mutants

A-B, Dose-response curves showing recruitment of β-arr1 to the plasma membrane by CB_1R-WT (black circles), CB_1R-DAY (white diamonds), CB_1R-DRA (white circles), CB_1R-DAA (white squares) or CB_1R-AAY (white triangles) in CHO cells under basal and different WIN55- (A) or 2-AG- (B) stimulated conditions, as detected by BRET

836 between β-arr1-Rluc and MP-mVenus. 0% reflects total inactivity of receptors, achieved
837 by inverse agonist treatment (AM251, 10 μM), and 100% reflects maximal WIN55- (A)
838 or 2-AG- (B) induced response (E_{max}) of CB_1R-AAY. Data are mean±SEM, n=3.
839 *p<0.05 vs vehicle treatment.
840
841 **Fig.7 Bias analysis showing functional selectivity of CB_1R mutants**
842 A-B, Equimolar comparison of CB_1R-WT (black points), CB_1R-DAA (grey squares) and
843 CB_1R-AAY (white triangles) functions. For each receptor, responses from G protein and
844 β-arr2 BRET dose-response curves, elicited by the same WIN55 (A) or 2-AG (B)
845 concentration, were plotted against each other. The left- and upward shift of CB_1R-AAY
846 points represents bias toward β-arr2 recruitment, whereas the downward shift of CB_1R-
847 DAA points indicates G protein bias. Data are mean±SEM. C, Equiactive comparison of
848 CB_1R-WT, CB_1R-DAA and CB_1R-AAY functions. The biased factor (β) was calculated
849 for each receptor, based upon EC_{50} and E_{max} values of G protein and β-arr2 BRET dose-
850 response curves obtained with WIN55 (black bars) or 2-AG (grey bars) stimuli, using the
851 equation described in *Materials and methods*. CB_1R-WT was used as reference receptor.
852 Positive values indicate bias towards G protein signaling, whereas negative values reflect
853 β-arrestin bias. Data are mean ± SD.
854
855 **Fig.8 Functional assays measuring intracellular signaling of wild-type and mutant**
856 **CB_1R variants**
857 A, Dose-response curves showing the inhibition of forskolin-induced cAMP
858 accumulation in CHO cells expressing CB_1R-WT, CB_1R-DAA or CB_1R-AAY under

basal and different WIN55-stimulated conditions, measured by the BRET changes of an EPAC-based intramolecular BRET sensor. BRET was measured 30 min after stimulus. 0% reflects total inactivity of receptors, achieved by inverse agonist treatment (AM251, 10 μM), and 100% reflects maximal WIN55-induced response (E_{max}) of CB_1R-WT. Data are mean±SEM, n=6. *p<0.05 vs basal state, #p<0.05 vs CB_1R-WT. B, Amounts of phosphorylated (pERK1/2) and total ERK1/2 proteins detected by Western blot in CHO cells expressing CB_1R-WT, CB_1R-DAA or CB_1R-AAY, after 0, 5 or 20 min of WIN55 (1 μM) treatment. Images are representative from four independent experiments. C, Quantification of Western blot data. 0% reflects background intensity, and 100% reflects WIN55-induced pERK1/2 intensity of CB_1R-WT at 5 min. Data are mean+SEM, n=4, *p<0.05 versus CB_1R-WT at 5 min, #p<0.05 versus CB_1R-WT at 20 min.

Supplementary Fig. 1 G protein activation of CB_1R-AAY mutant in HeLa cells

BRET measurements showing G_o protein activation of CB_1R-WT and CB_1R-AAY in HeLa cells under basal (white bars) and WIN55-stimulated (1 μM, black bars) conditions. 0% reflects total inactivity of receptors, achieved by inverse agonist treatment (AM251, 10 μM), and 100% reflects WIN55-induced response of CB_1R-WT. Data are mean±SEM, n=4. *p<0.05 vs basal, #p<0.05 vs CB_1R-WT.

Table 1. Parameters of G_o BRET and β-arrestin2 BRET dose-response curves for the different CB_1R variants

Bottom and E_{max} values are expressed as % of E_{max} of CB_1R-WT. Data are mean±SEM, n=3-8. *p<0.05 vs CB_1R-WT. n.d. – not detectable

882

883

884

Figure 1

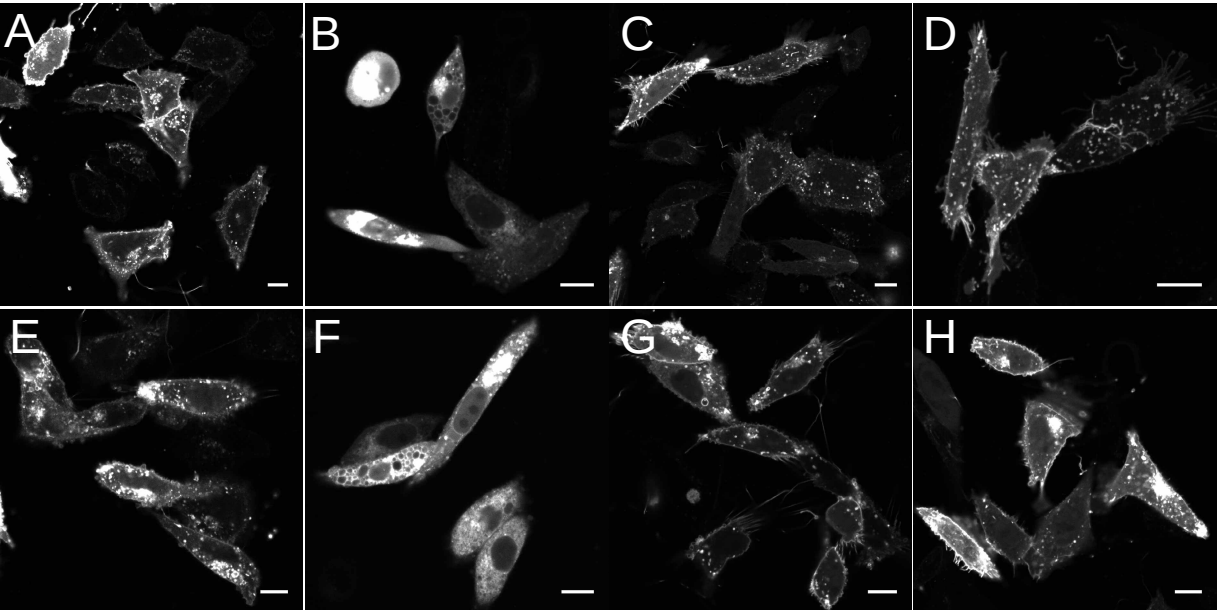
A
B
C
D
E
F
G
H

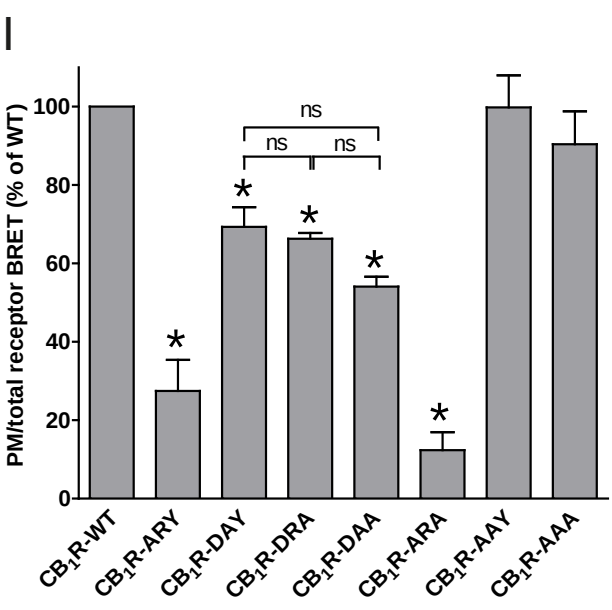
I
PM/total receptor BRET (% of WT)
100
80
60
40
20
0
ns
ns
ns
*
*
*
*
*
CB1R-WT
CB1R-ARY
CB1R-DAY
CB1R-DRA
CB1R-DAA
CB1R-ARA
CB1R-AAY
CB1R-AAA

Figure 2

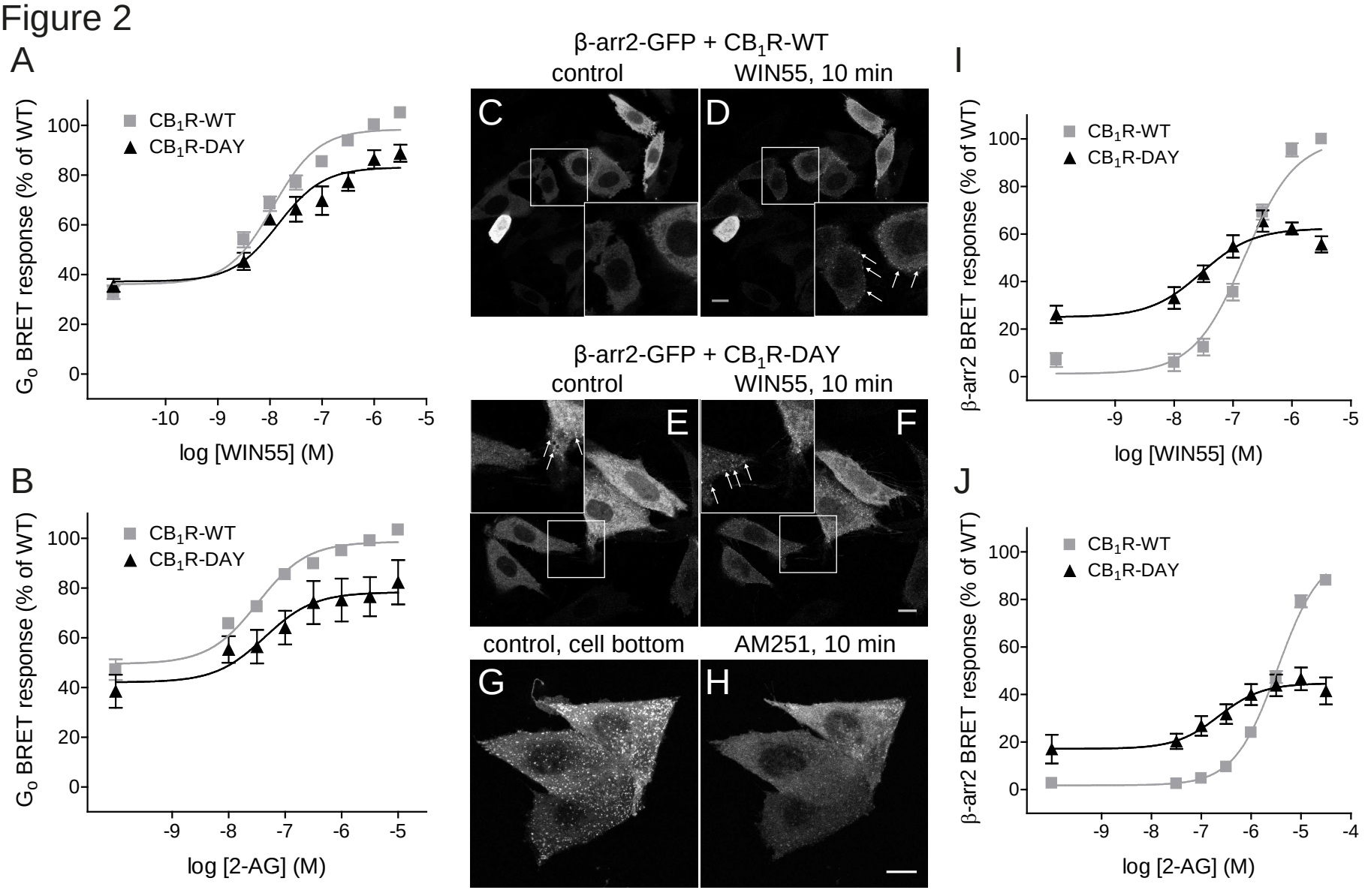
A
CB1R-WT
CB1R-DAY
Go BRET response (% of WT)
log [WIN55] (M)
B
CB1R-WT
CB1R-DAY
Go BRET response (% of WT)
log [2-AG] (M)
β-arr2-GFP + CB1R-WT
control
WIN55, 10 min
C
D
β-arr2-GFP + CB1R-DAY
control
WIN55, 10 min
E
F
control, cell bottom
AM251, 10 min
G
H
I
CB1R-WT
CB1R-DAY
β-arr2 BRET response (% of WT)
log [WIN55] (M)
J
CB1R-WT
CB1R-DAY
β-arr2 BRET response (% of WT)
log [2-AG] (M)

Figure 3

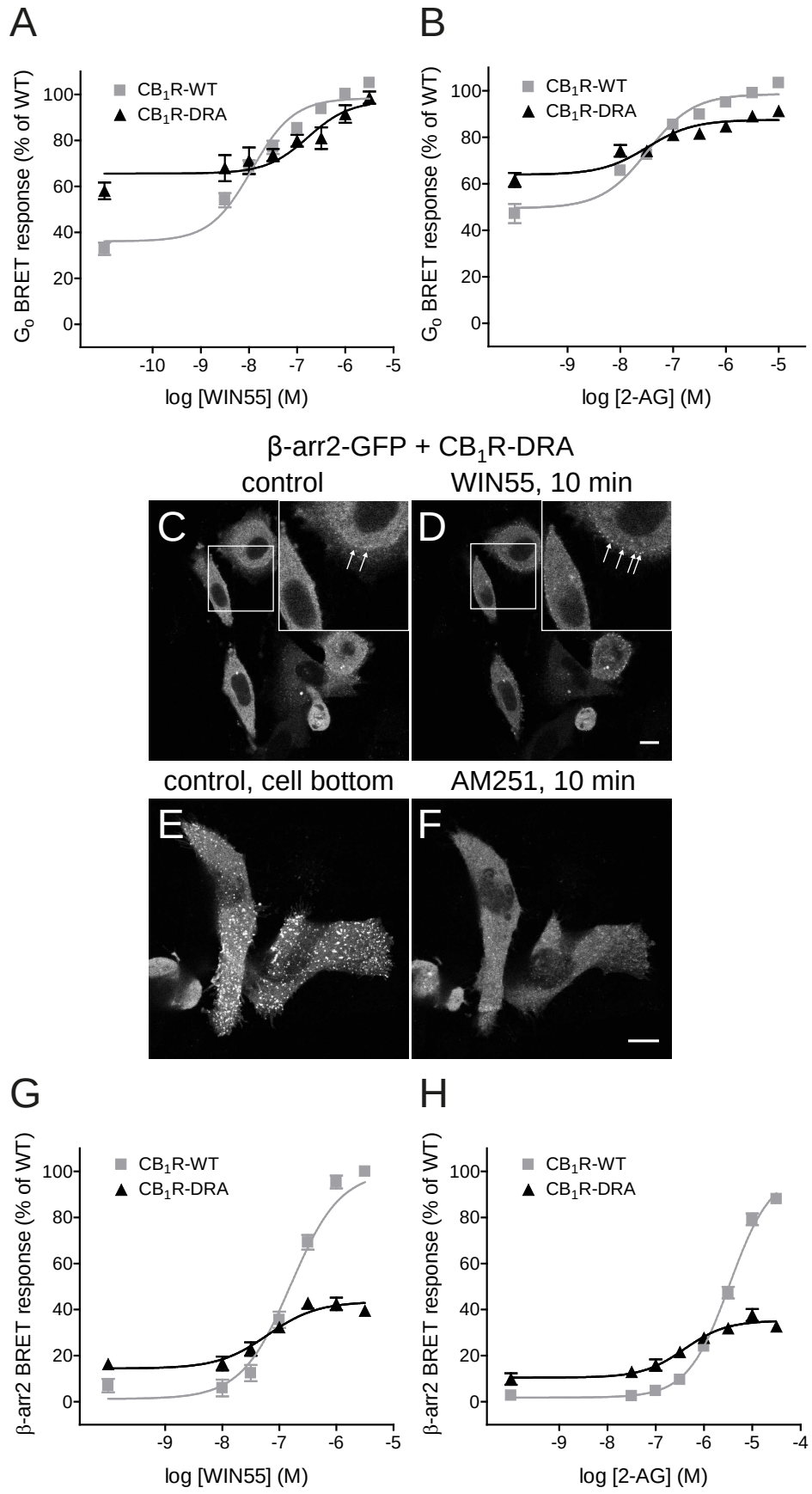
A
B
CB1R-WT
CB1R-DRA
G0 BRET response (% of WT)
log [WIN55] (M)
log [2-AG] (M)
β-arr2-GFP + CB1R-DRA
control
WIN55, 10 min
control, cell bottom
AM251, 10 min
C
D
E
F
G
H
β-arr2 BRET response (% of WT)

Figure 4

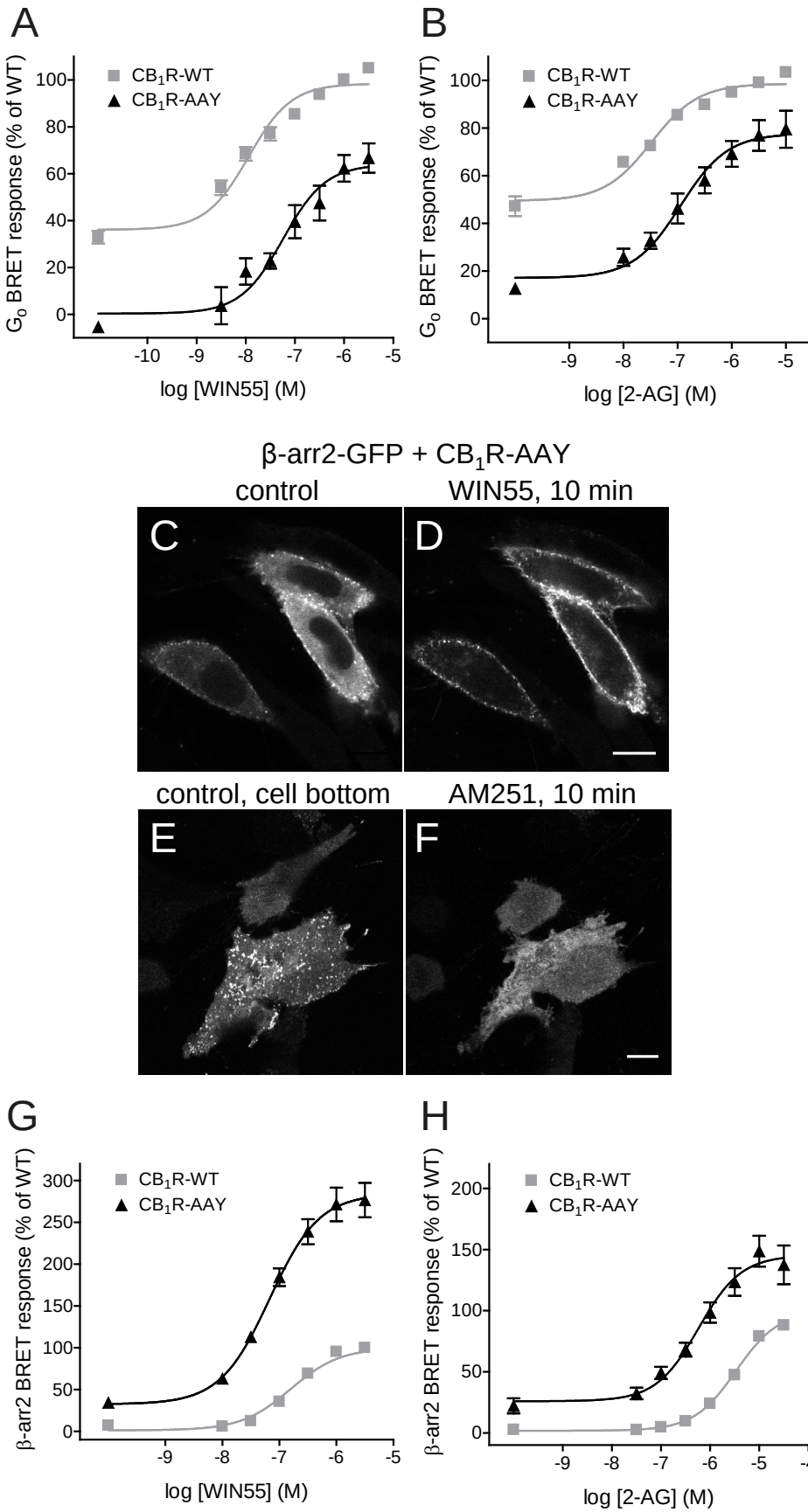
A
B
CB1R-WT
CB1R-AAY
Go BRET response (% of WT)
log [WIN55] (M)
log [2-AG] (M)
β-arr2-GFP + CB1R-AAY
control
WIN55, 10 min
control, cell bottom
AM251, 10 min
C
D
E
F
G
H
β-arr2 BRET response (% of WT)

Figure 5

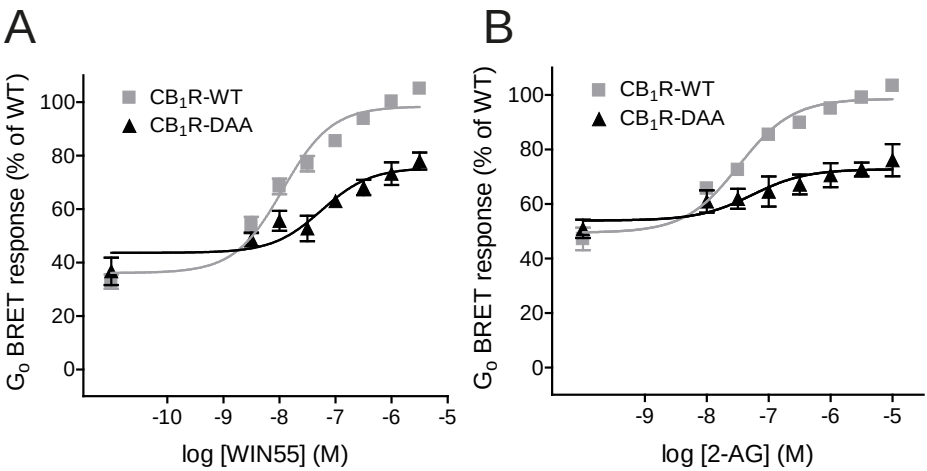
A
B
CB1R-WT
CB1R-DAA
Go BRET response (% of WT)
log [WIN55] (M)
log [2-AG] (M)

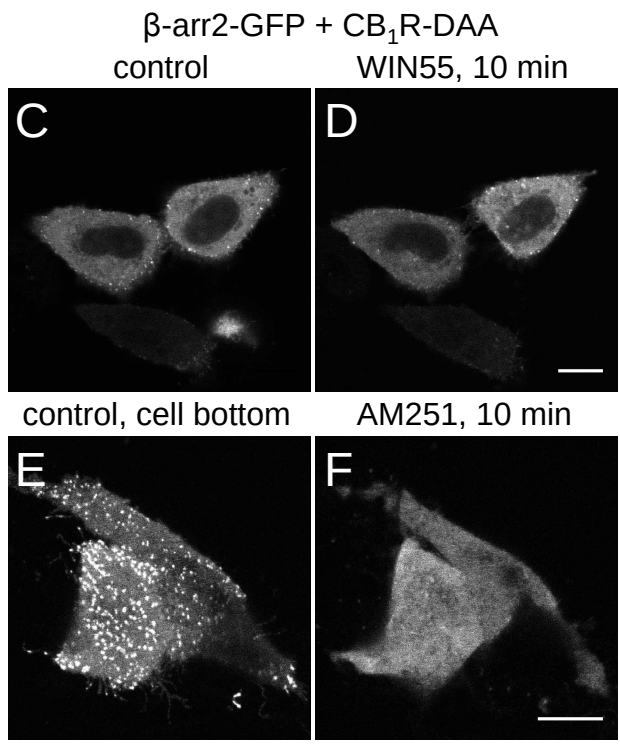
β-arr2-GFP + CB1R-DAA
control
WIN55, 10 min
C
D
control, cell bottom
AM251, 10 min
E
F

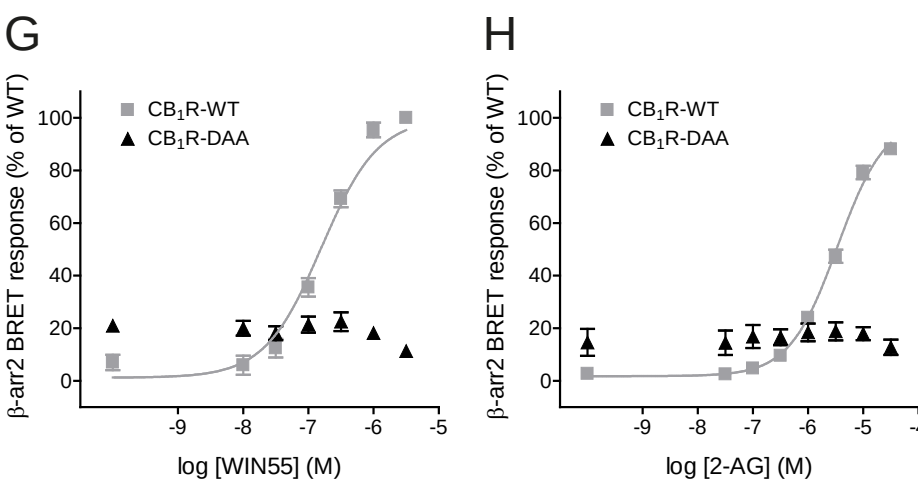
G
H
CB1R-WT
CB1R-DAA
β-arr2 BRET response (% of WT)
log [WIN55] (M)
log [2-AG] (M)

Figure 6

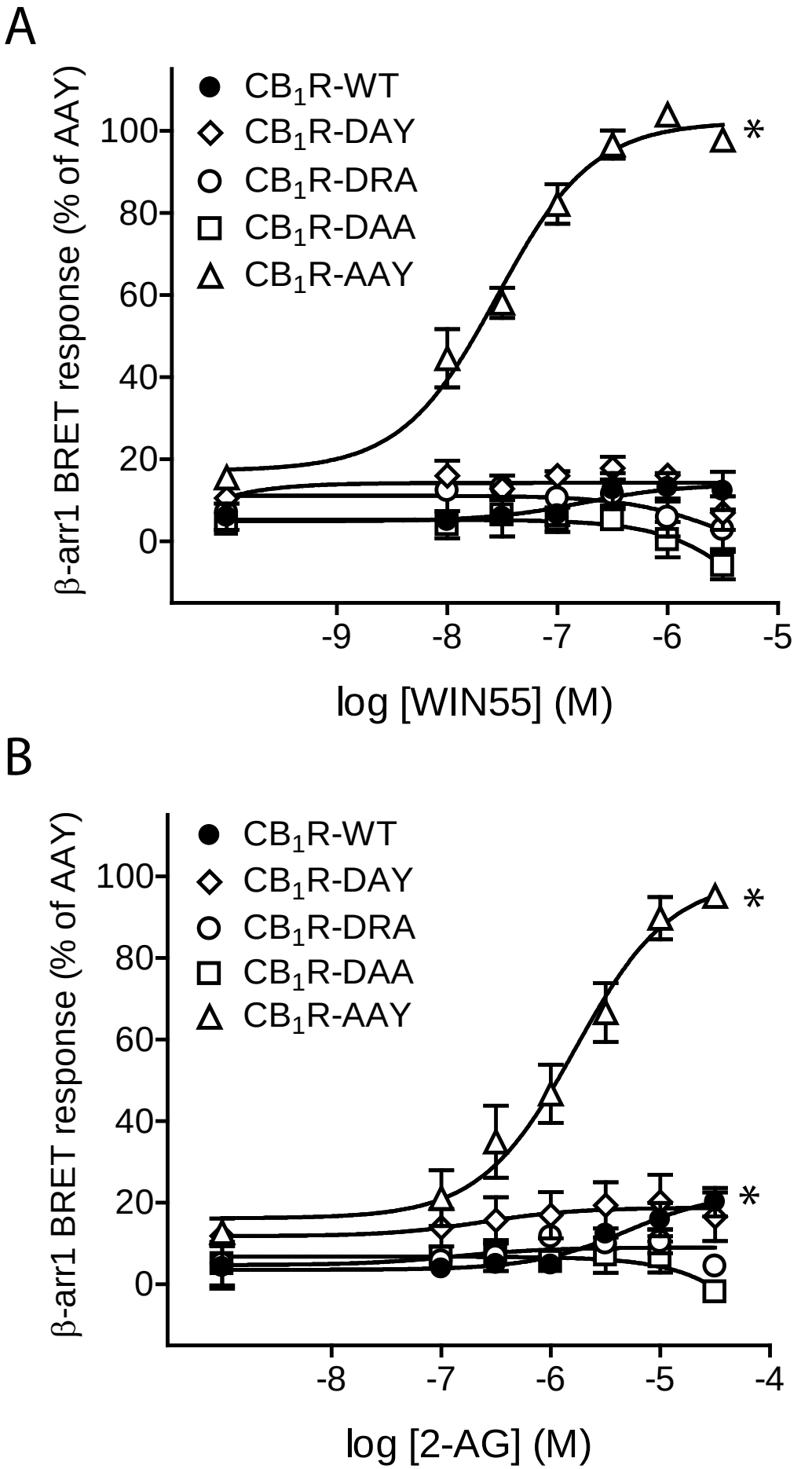
A
CB1R-WT
CB1R-DAY
CB1R-DRA
CB1R-DAA
CB1R-AAY
β-arr1 BRET response (% of AAY)
100
80
60
40
20
0
*
-9
-8
-7
-6
-5
log [WIN55] (M)
B
CB1R-WT
CB1R-DAY
CB1R-DRA
CB1R-DAA
CB1R-AAY
β-arr1 BRET response (% of AAY)
100
80
60
40
20
0
*
*
-8
-7
-6
-5
-4
log [2-AG] (M)

Figure 7

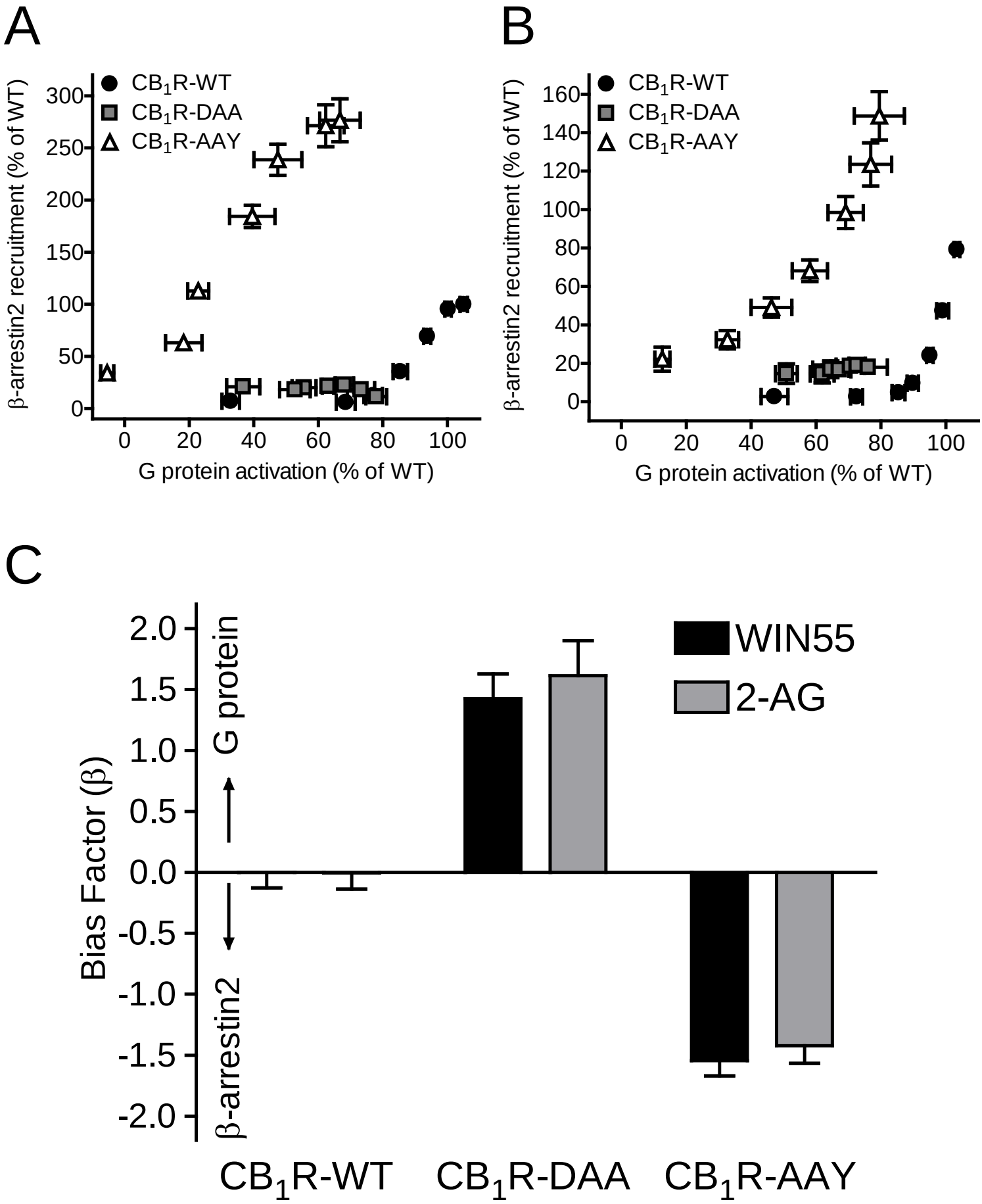
A
B
C
CB1R-WT
CB1R-DAA
CB1R-AAY
β-arrestin2 recruitment (% of WT)
G protein activation (% of WT)
Bias Factor (β)
G protein
β-arrestin2
WIN55
2-AG
CB1R-WT
CB1R-DAA
CB1R-AAY

Figure 8

A

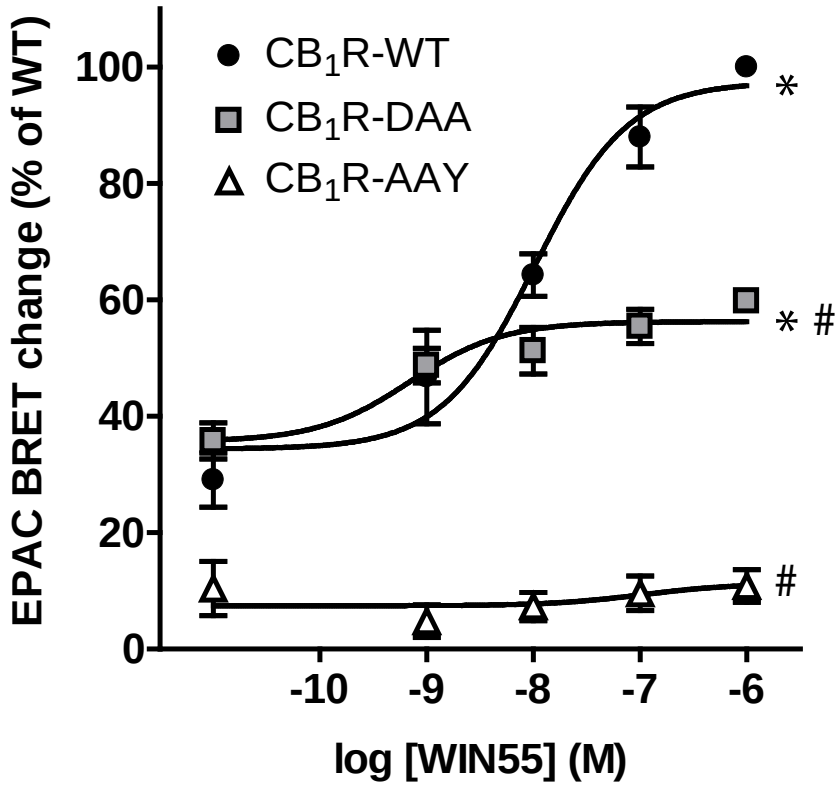
CB1R-WT
CB1R-DAA
CB1R-AAY
EPAC BRET change (% of WT)
100
80
60
40
20
0
-10
-9
-8
-7
-6
log [WIN55] (M)
*
* #
#

B

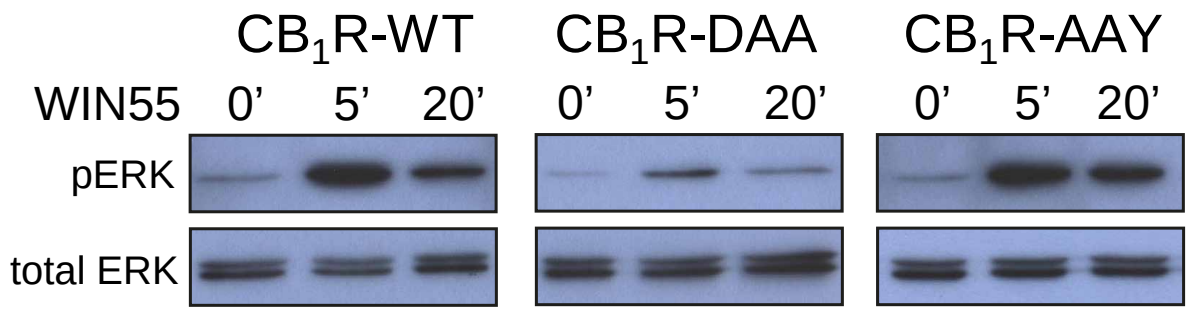
CB1R-WT
CB1R-DAA
CB1R-AAY
WIN55
0'
5'
20'
0'
5'
20'
0'
5'
20'
pERK
total ERK

C

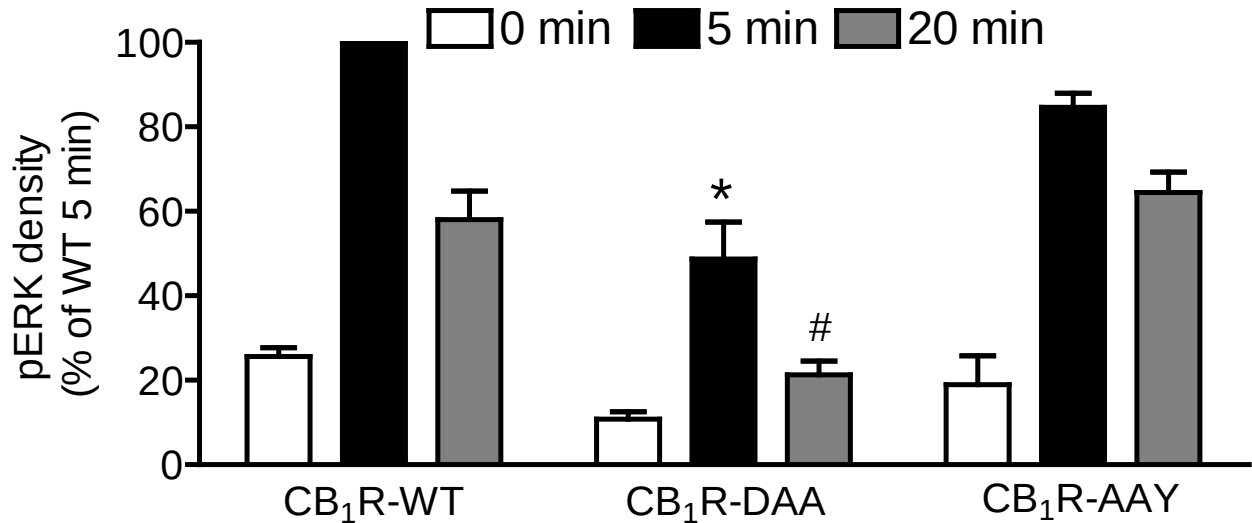
0 min
5 min
20 min
pERK density
(% of WT 5 min)
100
80
60
40
20
0
*
#
CB1R-WT
CB1R-DAA
CB1R-AAY

Table 1

	G_o BRET					
	WIN55			2-AG		
Receptor	pEC_{50}	bottom	E_{max}	pEC_{50}	bottom	E_{max}
CB_1R-WT	-7.89±0.07	36.85±2.47	100	-7.43±0.07	50.11±2.18	100
CB_1R-DAY	-7.85±0.17	37.19±3.95	83.12±3.95*	-7.36±0.34	42.11±6.35	78.31±4.10*
CB_1R-DRA	-6.78±0.27*	65.58±2.62*	97.22±4.31	-7.49±0.18	63.90±2.28*	87.49±1.35*
CB_1R-DAA	-7.25±0.23	43.62±2.86	75.45±2.92*	-7.26±0.39	53.99±3.56	72.79±2.48*
CB_1R-AAY	-7.24±0.17*	0.36±4.24*	64.06±4.43*	-6.95±0.15*	17.12±4.02*	77.69±3.52*

	β-arr2 BRET					
	WIN55			2-AG		
Receptor	pEC_{50}	bottom	E_{max}	pEC_{50}	bottom	E_{max}
CB_1R-WT	-6.80±0.051	1.23±2.53	100	-5.47±0.02	1.79±0.87	100
CB_1R-DAY	-7.53±0.19*	25.13±3.77*	62.36±2.60*	-6.65±0.28*	17.15±3.64*	44.72±2.71*
CB_1R-DRA	-7.21±0.16*	14.43±2.09*	43.46±1.84*	-6.41±0.16*	10.47±1.69*	35.22±1.52*
CB_1R-DAA	> -5.0*	20.96±2.35*	n.d.	> -4.5*	14.62±5.10*	n.d.
CB_1R-AAY	-7.17±0.10*	32.68±10.90*	284.10±9.93*	-6.24±0.14*	25.91±6.44*	145.30±6.74*

Supplementary Figure 1